All-Metal Endfire Antenna With High Gain and Stable Radiation Pattern for the Platform-Embedded Application

Yuefeng Hou, *Student Member, IEEE*, Yue Li, *Senior Member, IEEE*, Zhijun Zhang, *Fellow, IEEE*, and Magdy F. Iskander, *Life Fellow, IEEE*

***Abstract*— This paper presents a novel high-gain endfire slot antenna array fed by air-substrate microstrip line. It has a simple and compact structure consisting of a copper strip and two copper sheets. Designed based on the slot antenna array, the antenna could be embedded into a large metallic platform. The surface wave above the antenna radiates the energy to free space. Fed by the air-substrate microstrip line, the antenna works on the TEM mode. Therefore, the antenna obtains a suitable phase constant to realize stable endfire radiation pattern and could be designed by a long structure to realize high endfire gain. Because all of the antennas are designed by metal, it has the characteristics of high strength, easy fabrication, and low cost. With the radiating aperture of 3.5 wavelength, the antenna achieves a measured endfire gain of 11.81 dBi. The measured 1 and 3 dB gain bandwidths reach 4.5% and 8.4%, respectively. Good matching and stable endfire radiation pattern are obtained over the entire operating band from 3.75 to 4.15 GHz.**

***Index Terms*— Endfire, high endfire gain, platform embedded, slot array.**

I. Introduction

RECENTLY, due to the growing demand on the application of high-speed moving objects, the endfire antennas mounted on a large conducting plane have been investigated popularly. To decrease the aerodynamic drag, in the open literature, the antennas aimed to realize low profile [1]–[10] or even be platform embedded into a large metallic platform [11], [12].

Comparing with the endfire antennas with the horizontal polarization [13], the antennas with the vertical polarization could be mounted on a conducting plane directly. Therefore, most of the endfire antennas mounted on a large conducting plane were designed with the vertical polarization. To realize the low profile or to be platform embedded into a large metallic platform, the types of the radiating elements play a very important role. Monopole [1]–[3], [14], monocone [4], planar inverted-L antenna [5], half-mode cavity [6], half-mode dielectric waveguide [7]–[11], and slot [12], [15]–[20] have been widely used in endfire antennas.

For the monopole antenna, it needs the height of about one-quarter wavelength to achieve resonant [14], which is too high for the low-profile endfire antenna. Therefore, top-hat monopole antenna and folded top-hat monopole antenna were adopted in Yagi antenna [1] or log-periodic antennas [2], [3] to realize low profile. Among them, the antenna in [3] was designed with structurally conformal. Moreover, the antenna in [3] could be platform embedded into a conducting cylinder. However, the surrounding of the monopole antenna could not be sheltered by metal; otherwise the performance of the monopole antenna would be influenced seriously. Therefore, the endfire antenna with the radiating element of monopole antenna might make the structure of metallic platform complex. Monocone antenna has wider bandwidth compared with the monopole antenna. A Yagi antenna with the radiating element of the monocone antenna was designed to realize wideband [4]. Planar inverted-L antenna and half-mode cavity have low-profile structure, and they were applied in leaky-wave antenna [5] and Yagi antenna [6], respectively. However, if the antennas in [4]–[6] are attempted to be embedded into a metallic platform, they would have the similar problem as [3].

Half-mode dielectric waveguide is a continuous structure. On the one hand, it could be one part of a radiating structure to improve the bandwidth or the gain of the horn antennas [7], [8] and the multiresonant patch antenna [9]. On the other hand, it could be a radiating structure alone as the surface-wave antennas [10], [11]. Up to now, it was found that among the antenna radiated by the half-mode dielectric waveguide, only the surface-wave antenna in [11] was designed to be platform embedded into on a large metallic platform. The antenna in [11] used a gradient dielectric slab, which gradually became thinner along the propagation direction, to avoid the shelter of the metallic platform. However, the antenna in [11] has a large feed structure and a wide transverse dimension, which leads to an incompact structure. Moreover, the antenna in [11] is designed for the wideband application. The endfire gain of the antenna is relatively low because only part of the aperture is radiated at single-frequency point.

Manuscript received June 24, 2018; revised September 5, 2018; accepted September 27, 2018. Date of publication November 9, 2018; date of current version February 5, 2019. This work was supported by the National Natural Science Foundation of China under Contract 61525104. *(Corresponding author: Zhijun Zhang.)*

Y. Hou, Y. Li, and Z. Zhang are with the Beijing National Research Center for Information Science and Technology, Tsinghua University, Beijing 100084, China (e-mail: zjzh@tsinghua.edu.cn).

M. F. Iskander is with the Hawaii Center for Advanced Communications, University of Hawai'i at Mānoa, Honolulu, HI 96822 USA (e-mail: iskander@spectra.eng.hawaii.edu).

Color versions of one or more of the figures in this paper are available online at http://ieeexplore.ieee.org.

Digital Object Identifier 10.1109/TAP.2018.2879822

Compared with the radiating elements mentioned earlier, slot antennas are more suitable for platform embedded. Because they could be designed on a conducting plane and the feed structure could be embedded into the metallic platform. Among the endfire antennas radiated by slots which have been exhibited, there were two types of endfire antennas. One type was the substrate integrated waveguide (SIW) leaky-wave antennas with transverse slots [15]–[17], and the other type was the cavity-backed slot antennas [12], [18]–[20]. The SIW leaky-wave antennas could achieve endfire radiation pattern. However, the antennas in [15]–[17] are designed for beam scanning. The beam direction is sensitive to the frequency because the antennas work on the TE_{10} mode. The cavity-backed slot antennas in [12] and [18]–[20] are based on the principle of Yagi antenna. However, they have only three radiating elements leading to a sloping-upward beam and low endfire gain.

Based on the analysis mentioned earlier, it is a great challenge to realize an endfire antenna embedded into a metallic platform with high endfire gain and stable radiation pattern. So in this paper, a novel high-gain endfire slot antenna array fed by air-substrate microstrip line is proposed. The proposed antenna has a simple and compact structure which consists of one copper strip and two metal planes. Similar to the antenna in [12], several slots are notched on a conducting plane as the radiating aperture, and the feed structure is embedded into a metallic platform. So the antenna is suitable for platform-embedded application. However, the proposed antenna is fed by an air-substrate microstrip line. Therefore, the proposed antenna could be designed with a long structure and obtain a moderate phase constant. Compared with the antenna in [15]–[17], the proposed antenna could achieve a stable endfire radiation over the entire operating band. Compared with the antenna in [12] and [18]–[20], the proposed antenna could realize a high endfire gain. Moreover, all of the proposed antennas are designed by metal, so it has the characteristics of high strength, easy fabrication, and low cost. Finally, a simple prototype with the radiating aperture length of $3.5\lambda_0$ is fabricated to verify the new design method. The λ_0 is the wavelength at the center frequency of 4 GHz.

II. Antenna Design and Analysis

This paper aims to design an endfire antenna for the platform-embedded application. The endfire antenna should achieve high endfire gain and stable endfire radiation pattern. Meanwhile, the antenna should have a compact and all-metal structure. To realize the antenna mentioned above, the antenna is designed as a series-feed antenna. Because each radiating element of the series-feed antenna could be designed to radiate less energy [21], [22], compared with the other types of antennas, the series-feed antenna arrays are suitable to realize a long structure and a high gain with a relatively simple structure.

A. Element Design

When the slot antenna is placed on an infinite ground plane, the slot antenna has omnidirectional radiation pattern in the upper hemisphere. Therefore, the slot antenna is suitable to be designed as the radiating element of the endfire antenna. To design a radiating element which could be applied in the series-feed antenna and platform-embedded application, the evolvement of the proposed antenna element is shown in Fig. 1.

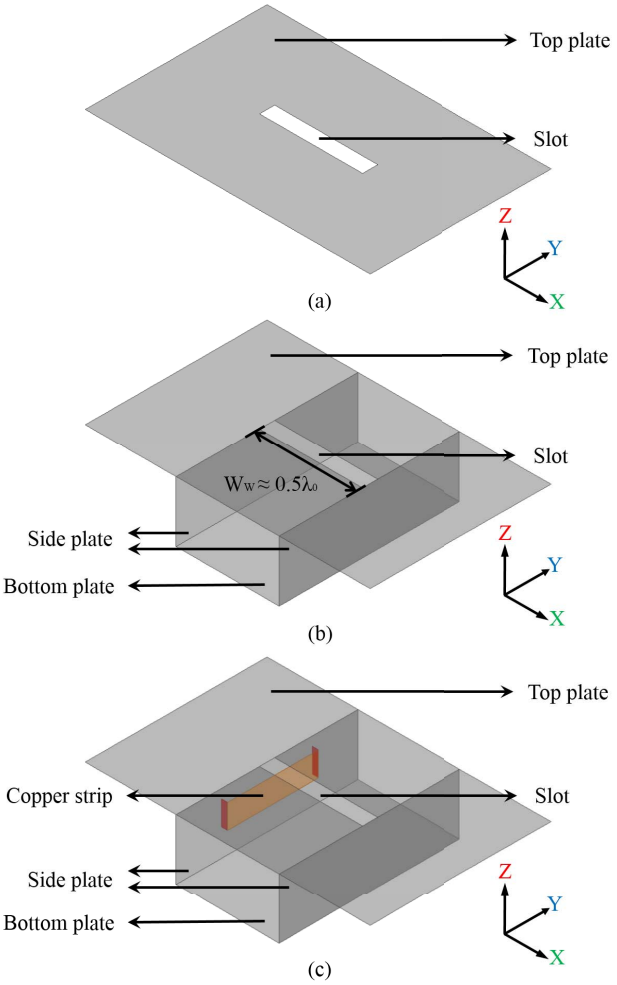

Fig. 1. Evolvement of the proposed antenna element. (a) Slot antenna. (b) Slot antenna with the half-open backed cavity. (c) Slot antenna with feed structure.

To begin with, as shown in Fig. 1(a), a slot is notched on a conducting plane. The conducting plane is regarded as the top plate in this paper. For the slot antenna in Fig. 1(a), it could radiate the energy to both the upper and the lower hemispheres.

Then, to restrict the slot antenna only radiating on the upper hemisphere, a half-open backed cavity is added under the slot antenna, as shown in Fig. 1(b). Because the structure in Fig. 1(b) is a part of a series-feed antenna array along the y-axis, the backed cavity could be not closed totally. The half-open backed cavity is formed by one bottom plate and two side plates, which could be bent by a piece of copper sheet. The length of the slot antenna is the same as the width of the backed cavity, which is about $0.5\lambda_0$.

Finally, a copper strip is added, as shown in Fig. 1(c). The copper strip and one of the side plates form an air-substrate

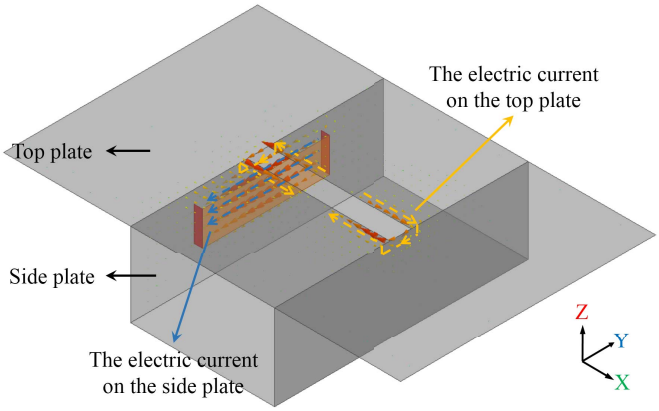

Fig. 2. Vector electric current distribution of the proposed antenna element at the center frequency of 4 GHz. Blue dashed line: electric current of microstrip line on the side plate. Yellow dashed line: electric current of the slot antenna on the top plate.

microstrip line, which is adopted to feed the slot antenna. The half-open cavity and the microstrip line are considered as a whole, which could be regarded as the feed structure of the radiating element. For the structure in Fig. 1(c), the slot antenna is designed on the top plate and the feed structure could be embedded into the metallic platform.

The microstrip line feeds the energy to the slot antenna by electrical current coupling. The vector electric current distribution on the top plate and the side plates is plotted in Fig. 2. When the microstrip line is fed, the electric current on the side plate close to the copper strip is excited. The electric current on the side plate is along the propagation direction. When the slot antenna is resonant, electric current surrounds the slot and parts of the electric current along the propagation direction flows through the side plate. Because the electric currents excited by the microstrip line and the slot flow are along the same direction, the energy of the microstrip line could be coupled by the slot antenna.

B. Endfire Array Design

Based on the proposed radiating element in Fig. 1(c), a slot antenna array fed by air-substrate microstrip line is proposed. The antenna is composed of a copper strip and two copper sheets. One of the copper sheets is etched with several slots, and it is regarded as the top plate, as shown in Fig. 3(a). The other copper sheet is bended to form the half-open backed cavity which consists of a bottom plate and two side plates. The copper strip and the half-open backed cavity are considered as a whole, which is regarded as the feed structure, as shown in Fig. 3(b). The proposed antenna formed by the top plate and feed structure is shown in Fig. 3(c). The detailed dimensions of the antenna are given in Table I.

As shown in Fig. 3(a), there are 15 slots notched on the top plate. The dimension of the top plate is about $0.8\lambda_0$ larger than the bottom plate to imitate a big conducting plane. The slot array forms the radiating aperture of the antenna with the length of $3.5\lambda_0$. The distance between the two adjacent slot antennas is $0.25\lambda_0$, which is a self-matching condition

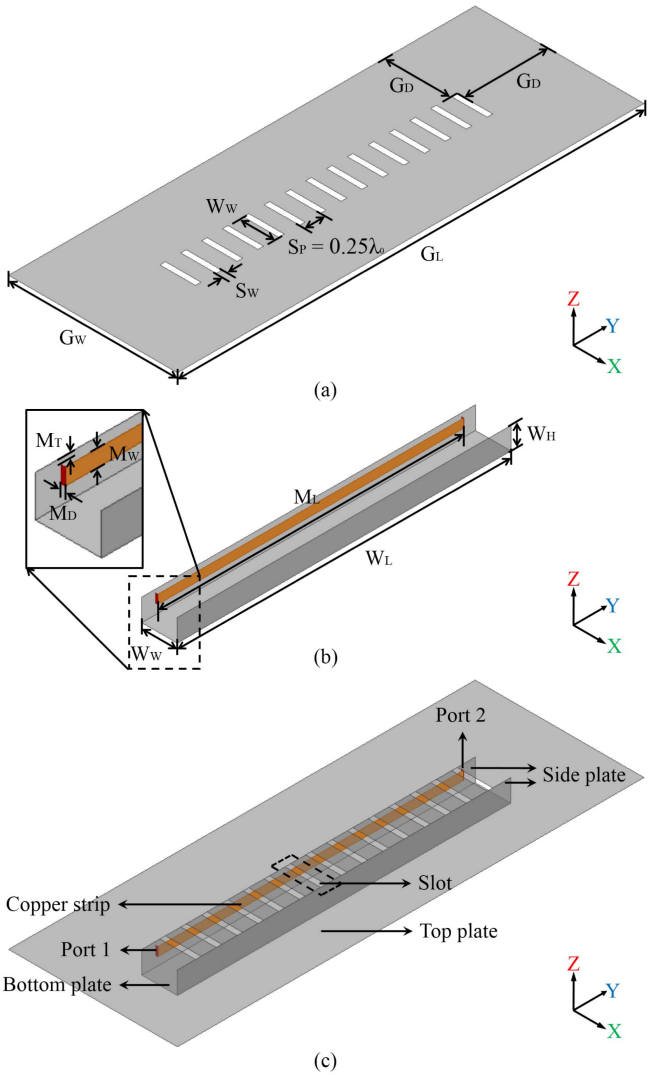

Fig. 3. Configuration of the slot antenna array fed by air-substrate microstrip line. (a) Top plate of the antenna. (b) Feed structure of the antenna. (c) Perspective view of the antenna.

TABLE I
DETAILED DIMENSION OF THE PROPOSED ANTENNA

Parameter	Value (mm)
S_W	5
S_P	18.75
M_L	275
M_W	8
M_D	2
M_T	3
W_L	300
W_W	32
W_H	20
G_L	420
G_W	152
G_D	60

because reflections from adjacent slots cancel each other out. As shown in Fig. 3(b), the width of the bottom plate and the length of the slot antenna are the same. To make the slot

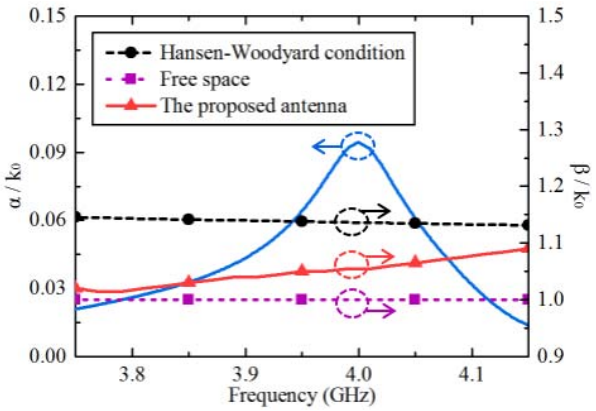

Fig. 4. Normalized leakage constant and normalized phase constant of the proposed antenna versus frequency.

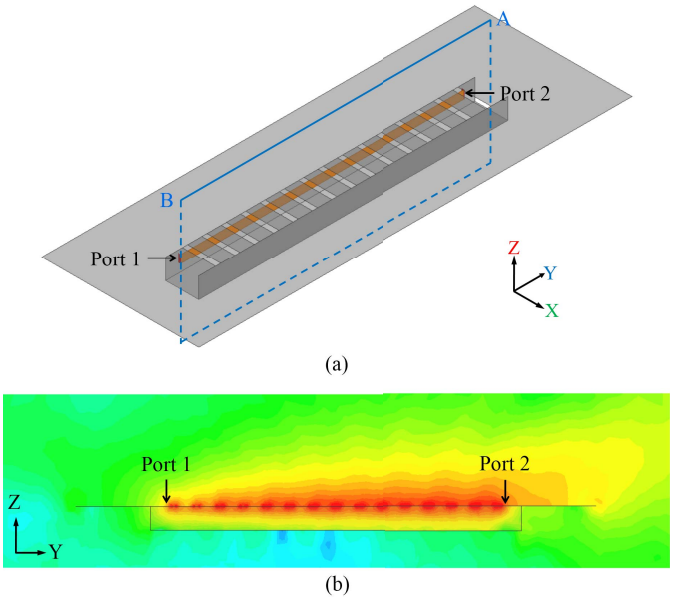

Fig. 5. Electric field magnitude distribution of the proposed antenna at the center frequency of 4 GHz. (a) Reference plane on the proposed antenna, which is the *yoz* plane through the reference line of *AB*. (b) Electric field magnitude distribution on the reference plane.

antenna obtains a good radiation capability, the height of the proposed antenna requires about $0.25\lambda_0$. The copper strip and the one of the side plates form the air-substrate microstrip line. The microstrip line is close to the top plate to feed the slot array. Each slot antenna can couple part of the energy from the microstrip line by coupling of electrical current.

However, the top plate and the half-open backed cavity might form a waveguide which works on the TE_{10} mode. To suppress the propagation of the TE_{10} mode, the width of the half-open backed cavity is optimized to be less than $0.43\lambda_0$, which makes the waveguide an evanescent one over the entire operating band. By adjusting the width of the slots, the slot array keeps resonant at the center frequency of 4 GHz.

C. Propagation and Radiation Performance

To evaluate the performance, the leakage constant and phase constant of the antenna are presented. The normalized leakage constant (α/k_0) of the proposed antenna versus the frequency is shown in Fig. 4. Around the center frequency, due to the strong coupling between the slot array and the microstrip line, more energy in the microstrip line is coupled by slot array and then radiated to the free space, which leads to a higher leakage constants. Fig. 4 also exhibits the normalized phase constant (β/k_0) of the proposed antenna versus the frequency. As presented in [15], for the endfire antenna, the leaky mode becomes small and the surface-wave mode is the dominant mode. Therefore, to evaluate the radiation performance of the antenna, the phase constant should be obtained from the energy of the surface wave. Since the energy of the surface-wave mode is mainly outside of the antenna, the phase constant is sampled from the position above the top plate. As shown in Fig. 4, with the frequency increasing, the phase constant of the antenna is increasing gradually. However, the phase constant of the antenna is still similar to the phase constant of free space over the operating band from 3.75 to 4.15 GHz, which indicates that the antenna could realize stable endfire radiation.

The electric field magnitude distribution of the antenna at the center frequency of 4 GHz is shown in Fig. 5. The antenna is excited at the port 1. A reference plane is plotted in Fig. 5(a). It is the *yoz* plane through the reference line of AB. The electric field magnitude distribution on the reference plane is shown in Fig. 5(b). It is found that the slot array is surrounded by the strong energy of electric field which indicates that all the slot antennas contribute to the radiation. The field distribution verifies that the slot array has a good capability.

The simulated normalized radiation patterns of the E-plane and the H-plane at different frequencies are presented in Fig. 6(a) and (b), respectively. As shown in Fig. 6(a), due to the influence of the finite ground, the beam directions tilt upward. The main beam directions at 3.85, 4, and 4.15 GHz are 71°, 73°, and 77°, respectively. As shown in Fig. 6(b), the half-power beam widths (HPBW) at 3.85, 4, and 4.15 GHz are 39°, 35°, and 28°, respectively. From Fig. 6, all of the front-to-back radios (FTBRs) at the three frequency points are higher than 10 dB. The moderate beam direction, HPBW, and FTBR verify the antenna having a good and stable endfire radiation pattern over the entire operating bandwidth.

D. Parameter Optimization

The distance M_T between the copper strip and the top plate is adjusted to investigate the effect of the parameters to the antenna. As shown in Fig. 7, when the distance is adjusted, the level of the transmission coefficient and the center frequency change at the same time. When the distance varies from 1 to 4 mm, the minimum level of the transmission coefficient is -12, -21.5, and -11 dB, respectively. The center frequency of the antenna decreases from 4.05 to 3.95 GHz with the distance increasing from 1 to 4 mm. From Fig. 7, it is also found that the reflection coefficient has little change when the distance between the copper strip and the top plate is adjusted. Therefore, if the antenna is designed with a longer

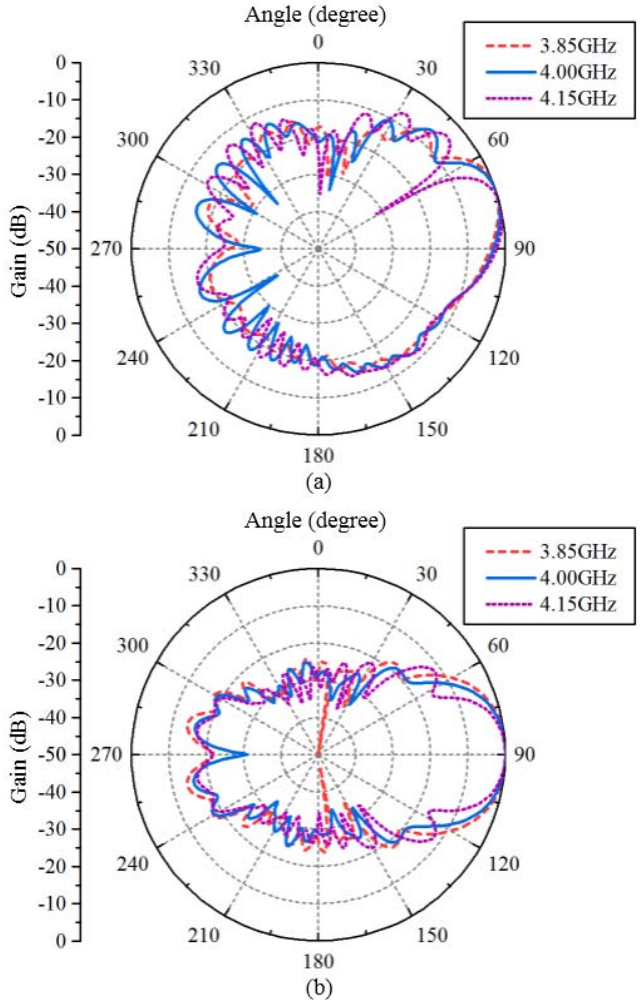

Fig. 6. Simulated normalized radiation patterns at different frequencies in (a) E-plane (*yoz* plane) and (b) H-plane (*xoy* plane).

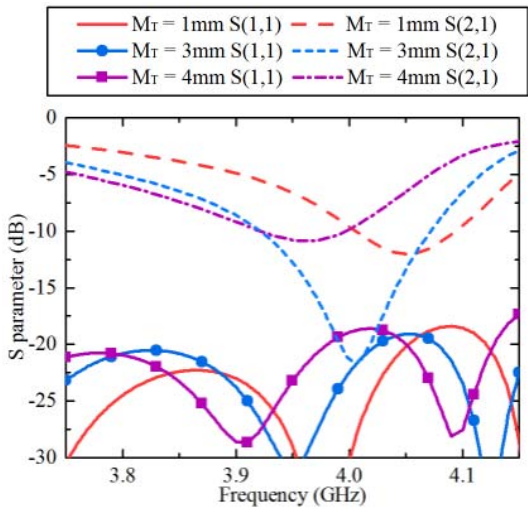

Fig. 7. Simulated S-parameters of the proposed antenna with different M_T.

structure to realize a higher endfire gain, the distance M_T is an important parameter to keep the antenna maintaining a good radiation capability.

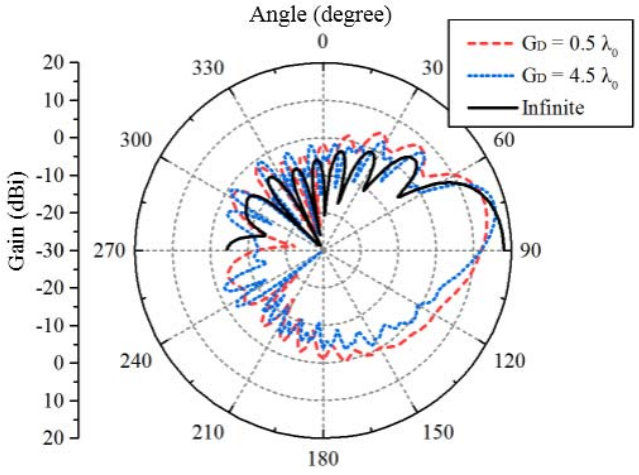

Fig. 8. Simulated radiation patterns at the center frequency of 4 GHz in the E-plane (*yoz* plane) with a different G_D.

The radiation patterns of the antenna with different sizes of the top plate at the center frequency are shown in Fig. 8. The G_D is the distance between the edge of the top plate and the edge of the bottom plate, as shown in Fig. 3(a). With the dimension of the top plate increasing, the beam direction varies from 73° to 75°. At different dimensions of the top plate, the values of the FTBR keep better than 20 dB and the values of the endfire gain are almost unchanged. If the antenna is designed with infinite ground plane, the beam direction is endfire and the sidelobe is lower, as shown in Fig. 8. The endfire gain of the antenna with infinite ground plane is about 6 dB higher than the antenna with finite ground plane.

III. Fabrication and Measured Results

A prototype is fabricated and measured to provide a verification of the new design method. Geometry of the corresponding slot antenna array is shown in Fig. 9. The antenna is composed of a copper strip, two copper sheets, and two coaxial lines. The copper strip and the copper sheets are designed by 0.5 mm-thick line-cutting copper plates. One of the copper sheets is bended to form the side plates and the bottom plate of the antenna. The other copper sheet is notched 15 grooves to form the top plate. As shown in Fig. 7, the position of the copper strip has an effect on the performance of the proposed antenna. However, the weight of the copper strip is light because of the narrow-width structure. Therefore, the copper strip could be fastened on the copper sheet easily. As presented in Fig. 9(a), to fasten the copper strip tightly, the foam with the height of 2 mm is under the copper strip as support, and a wide tape is adopted to fasten the copper strip and foam on the copper sheet stably. The copper strip and part of the copper sheet realize an air-substrate microstrip line. The microstrip line is connected to the coaxial lines on both ends. To mitigate the effect of the discontinuities between the microstrip line and the coaxial lines, isosceles trapezoid structures are added between them. One side of the isosceles trapezoid structure has the same width as the copper strip, which is 8 mm. The other side of the isosceles trapezoid structure is with the width of 6 mm. The antenna is excited at the port 1. The port

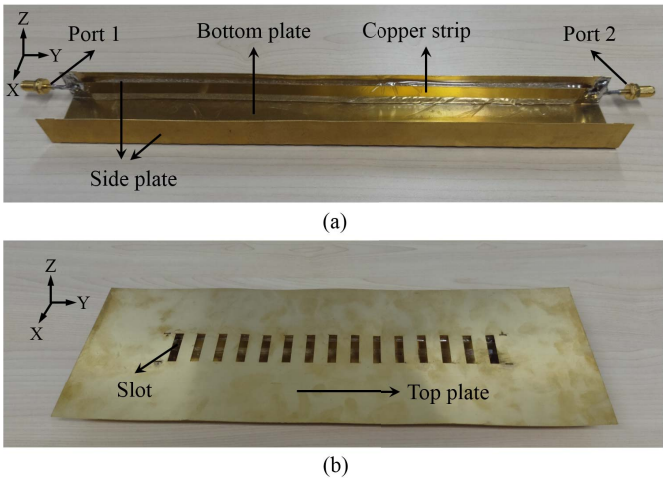

Fig. 9. Fabricated prototype of the proposed antenna. (a) Feed structure of the proposed antenna. (b) Whole proposed antenna.

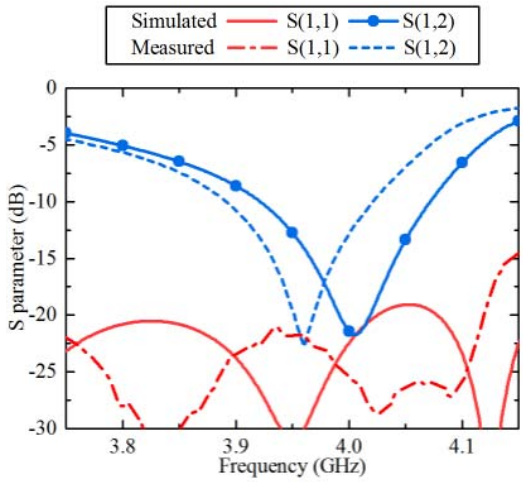

Fig. 10. Simulated and measured S-parameters of the proposed antenna.

2 is terminated with a match load. The S-parameters were measured using a N5071B vector network analyzer (300 kHz to 9 GHz); the gains and radiation patterns were measured in a far-field anechoic chamber.

The simulated results are based on the model shown in Fig. 3(c). The simulated and measured S-parameters of the antenna are shown in Fig. 10. Both the simulated and measured S-parameters are lower than −10 dB, which indicates that good matching is achieved over the operating band from 3.75 to 4.15 GHz. The simulated and the measured transmission magnitude are both the lower than −20 dB at the frequency of 4 and 3.95 GHz, respectively. The low level of the transmission coefficient indicates that the antenna has a good radiation efficiency.

The simulated and measured normalized radiation patterns of the E-plane and the H-plane are illustrated in Fig. 11. The simulated and the measured radiation patterns are presented at 4 and 3.95 GHz, respectively. As shown in Fig. 11(a), due to the existence of the finite ground plane, the simulated and measured radiation beam angle in the E-plane are about 17° and 19° away from the endfire direction, respectively. In the H-plane, the HPBW of both the simulated and measured

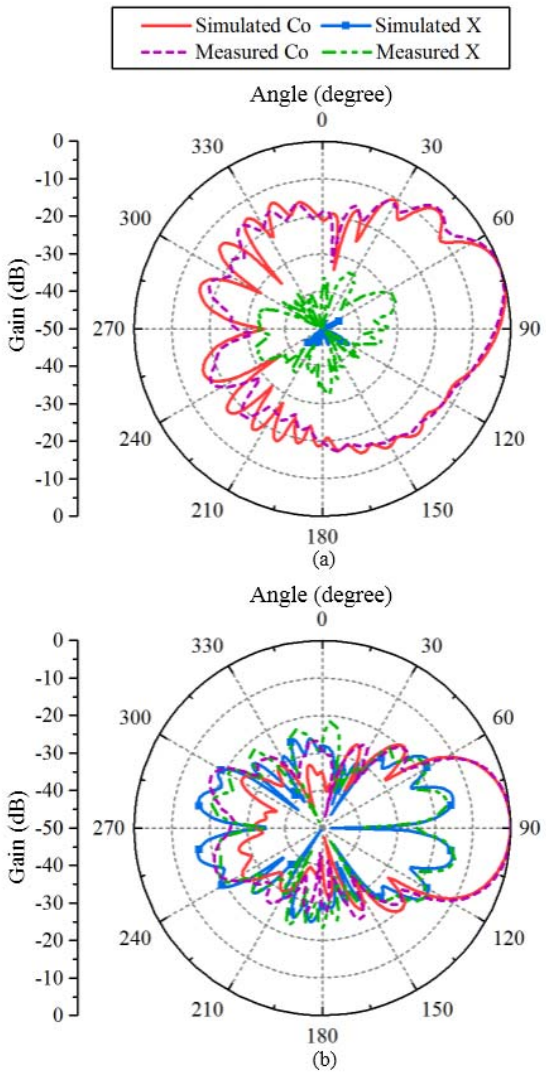

Fig. 11. Simulated and measured normalized radiation patterns of the proposed antenna in (a) E-plane (*yoz* plane) and (b) H-plane (*xoy* plane). The simulated radiation patterns are presented with 4 GHz, and the measured radiation patterns are presented with 3.95 GHz, respectively.

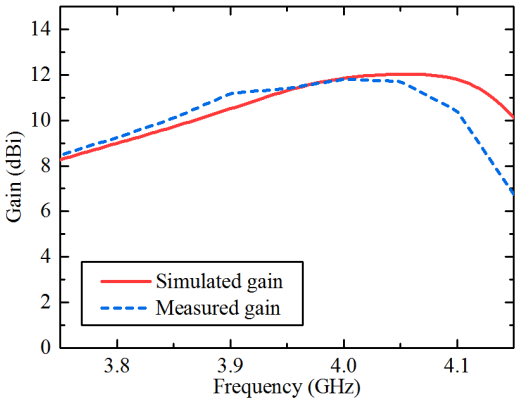

Fig. 12. Simulated and measured endfire gains of the proposed antenna.

radiated pattern is nearly 35° as presented in Fig. 11(b). The antenna has a high level of FTBR and a low level of cross polarization at the center frequency. The simulated and measured FTBR are 32.5and 25 dB, respectively. The

TABLE II
COMPARISON BETWEEN THE ENDFIRE ANTENNAS IN THE OPEN LITERATURE AND THE PROPOSED ANTENNA (NG: NOT GIVEN)

Ref.	Length (λ_0)	Width (λ_0)	Height (λ_0)	Dielectric (ε_r)	Max. Endfire Gain (dBi)	-1dB Endfire Gain BW (%)	3dB Endfire Gain BW (%)	Platform Embedded
[5]	6.10	0.39	1/53	1	11.5	4.0	7.0	×
[6]	2.97	1.10	1/35	2.33	10.4	3.7	7.6	×
[9]	2.41	1.93	1/8.7	2.1	9.70	7.9	15.8	×
[14]	5.67	0.34	1/4.7	1	13.3	8.0	17.0	×
[3]	5.80	2.00	1/6.2	3.38	≈ 6.0	NG	NG	√
[11]	10.87	4.67	1/2.5	2.2	≈ 10.0	NG	NG	√
[18]	1.09	0.61	1/20	2.1	≈ 4.5	NG	NG	√
[20]	0.93	0.62	1/17	3.66	≈ 2.5	NG	NG	√
This work	3.50	0.43	1/3.8	1	11.8	4.5	8.4	√

simulated and measured cross polarization are about 48 and 30 dB lower than co polarization. Therefore, a good endfire radiation pattern is obtained by the proposed antenna.

Fig. 12 shows the simulated and measured endfire gains of the antenna. The simulated endfire gain is better than 10 dBi from 3.87 to 4.15 GHz with the maximum value of 12.04 dBi at the frequency of 4.05 GHz. The measured endfire gain is better than 10 dBi from 3.84 to 4.11 GHz with a maximum value of 11.81 dBi at the frequency of 4 GHz. The simulated 1 and 3 dB gain bandwidths could reach 4.9% and 9.1%, respectively. The measured 1 and 3 dB gain bandwidths could reach 4.5% and 8.4%, respectively. It is found that the bandwidth of the proposed antenna is relatively narrow. The bandwidth requires to be broaden in the future.

The slight difference between the simulated and measured results may be attributed to the missing consideration about the influence of the isosceles trapezoid structures, and the fabrication and assembly errors. However, it still indicates that good agreement between the simulated and measured results.

Table II presents a comparison between the endfire antennas in the open literature and the proposed antenna. The dimension of the antennas is calculated at the frequency where the antennas obtain the maximum endfire gain. As shown in Table II, compared with the endfire antennas ([5], [6], [9], [14]) which have a high endfire gain, the proposed antenna also has a high endfire gain. Meanwhile, the proposed antenna could be embedded into a metallic platform. Compared with the endfire antennas ([3], [11], [18], [20]) which could be applied in the platform-embedded applications, the proposed antenna has a narrower width, a higher endfire gain, and a higher strength.

Therefore, compared with the endfire antennas in the open literature, the most important advantages of the proposed antenna are high endfire gain, platform-embedded applications, and high strength. Moreover, the proposed antenna also has the advantages of stable endfire radiation pattern, easy fabrication, and low cost.

IV. CONCLUSION

This paper proposes a novel high-gain endfire slot antenna array fed by air-substrate microstrip line. The advantages of the antenna are listed as follows.

1) The antenna is designed on a conducting plane and the feed structure is embedded under the metallic platform. The structure could be easily integrated to platform-embedded applications.
2) The microstrip line with air media, which works on the TEM mode, has the required endfire phase constant and generates a stable endfire radiation pattern.
3) The antenna is a series-feed antenna, so it could be designed with a longer structure to realize a high endfire gain.
4) The antenna is designed as an all-metal structure, which has the characteristic of high strength, easy fabrication, and low cost.

Therefore, the antenna is suitable to be employed on applications of high-speed moving objects, such as aircraft, unmanned aerial vehicle, and missile.

REFERENCES

[1] Z. Hu, Z. Shen, W. Wu, and J. Lu, "Low-profile top-hat monopole Yagi antenna for end-fire radiation," *IEEE Trans. Antennas Propag.*, vol. 63, no. 7, pp. 2851–2857, Jul. 2015.
[2] Z. Hu, Z. Shen, W. Wu, and J. Lu, "Low-profile log-periodic monopole array," *IEEE Trans. Antennas Propag.*, vol. 63, no. 12, pp. 5484–5491, Dec. 2015.
[3] Q. Chen, Z. Hu, Z. Shen, and W. Wu, "2–18 GHz conformal low-profile log-periodic array on a cylindrical conductor," *IEEE Trans. Antennas Propag.*, vol. 66, no. 2, pp. 729–736, Feb. 2018.
[4] Y. Zhao, Z. Shen, and W. Wu, "Wideband and low-profile monocone quasi-Yagi antenna for end-fire radiation," *IEEE Antennas Wireless Propag. Lett.*, vol. 16, pp. 325–328, 2017.
[5] P. Liu, H. Feng, Y. Li, and Z. Zhang, "Low-profile endfire leaky-wave antenna with air media," *IEEE Trans. Antennas Propag.*, vol. 66, no. 3, pp. 1086–1092, Mar. 2018.
[6] J. Liu and Q. Xue, "Microstrip magnetic dipole yagi array antenna with endfire radiation and vertical polarization," *IEEE Trans. Antennas Propag.*, vol. 61, no. 3, pp. 1140–1147, Mar. 2013.
[7] Y. Zhao, Z. Shen, and W. Wu, "Wideband and low-profile H-plane ridged SIW horn antenna mounted on a large conducting plane," *IEEE Trans. Antennas Propag.*, vol. 62, no. 11, pp. 5895–5900, Nov. 2014.
[8] Y. Zhao, Z. Shen, and W. Wu, "Conformal SIW H-plane horn antenna on a conducting cylinder," *IEEE Antennas Wireless Propag. Lett.*, vol. 14, pp. 1271–1274, 2015.
[9] S. Zhang and G. F. Pedersen, "Compact wideband and low-profile antenna mountable on large metallic surfaces," *IEEE Trans. Antennas Propag.*, vol. 65, no. 1, pp. 6–16, Jan. 2017.
[10] Z. Chen and Z. Shen, "Wideband flush-mounted surface wave antenna of very low profile," *IEEE Trans. Antennas Propag.*, vol. 63, no. 6, pp. 2430–2438, Jun. 2015.
[11] P. Wang and Z. Shen, "End-fire surface wave antenna with metasurface coating," *IEEE Access*, vol. 6, pp. 23778–23785, 2018.
[12] Z. Chen and Z. Shen, "Conformal cavity-backed slot antenna embedded in a conical platform for end-fire radiation," in *IEEE Antennas Propag. Symp. Dig.*, Jul. 2017, pp. 2239–2240.
[13] P. Wang, G. Wen, H. Zhang, and Y. Sun, "A wideband conformal end-fire antenna array mounted on a large conducting cylinder," *IEEE Trans. Antennas Propag.*, vol. 61, no. 9, pp. 4857–4861, Sep. 2013.

[14] Y. Hou, Y. Li, Z. Zhang, and Z. Feng, "Narrow-width periodic leaky-wave antenna array for endfire radiation based on Hansen–Woodyard condition," *IEEE Trans. Antennas Propag.*, vol. 66, no. 11, pp. 6393–6396, Nov. 2018.
[15] J. Liu, D. R. Jackson, and Y. Long, "Substrate integrated waveguide (SIW) leaky-wave antenna with transverse slots," *IEEE Trans. Antennas Propag.*, vol. 60, no. 1, pp. 20–29, Jan. 2012.
[16] J. Liu, D. R. Jackson, Y. Li, C. Zhang, and Y. Long, "Investigations of SIW leaky-wave antenna for endfire-radiation with narrow beam and sidelobe suppression," *IEEE Trans. Antennas Propag.*, vol. 62, no. 9, pp. 4489–4497, Sep. 2014.
[17] J. Liu, W. Zhou, and Y. Long, "A simple technique for open-stopband suppression in periodic leaky-wave antennas using two nonidentical elements per unit cell," *IEEE Trans. Antennas Propag.*, vol. 66, no. 6, pp. 2741–2751, Jun. 2018.
[18] A. Y. Simba, M. Yamamoto, and K. Itoh, "Planar-type sectored antenna based on slot Yagi–Uda array," *IEE Proc.-Microw., Antenna Propag.*, vol. 152, no. 5, pp. 347–353, Oct. 2005.
[19] Z. Chen and Z. Shen, "A compact cavity-backed endfire slot antenna," *IEEE Antennas Wireless Propag. Lett.*, vol. 13, pp. 281–284, 2014.
[20] P. Rodriguez-Ulibarri and T. Bertuch, "Microstrip-fed complementary Yagi–Uda antenna," *IET Microw. Antennas Propag.*, vol. 10, no. 9, pp. 926–931, Jun. 2016.
[21] Y. Li, Z. Zhang, C. Deng, Z. Feng, and M. F. Iskander, "2-D planar scalable dual-polarized series-fed slot antenna array using single substrate," *IEEE Trans. Antennas Propag.*, vol. 62, no. 4, pp. 2280–2283, Apr. 2014.
[22] K. Wei, Z. J. Zhang, Z. H. Feng, and M. F. Iskander, "Periodic leaky-wave antenna array with horizontally polarized omnidirectional pattern," *IEEE Trans. Antennas Propag.*, vol. 60, no. 7, pp. 3165–3173, Jul. 2012.

Yuefeng Hou (S'16) received the B.S. degree from the University of Electronic Science and Technology of China, Chengdu, China, in 2015. He is currently pursuing the Ph.D. degree in electrical engineering with Tsinghua University, Beijing, China.

His current research interests include leaky-wave endfire antenna array, reduced massive MIMO antenna array, and metamaterial.

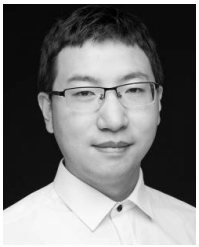

Yue Li (S'11–M'12–SM'17) received the B.S. degree in telecommunication engineering from Zhejiang University, Hangzhou, China, in 2007, and the Ph.D. degree in electronic engineering from Tsinghua University, Beijing, China, in 2012.

In 2010, he joined the Institute for Infocomm Research, A∗STAR, Singapore, as a Visiting Scholar. In 2012, he joined the Hawaii Center of Advanced Communication, University of Hawai'i at Mānoa, Honolulu, HI, USA. In 2012, he joined the Department of Electronic Engineering, Tsinghua University, as a Post-Doctoral Fellow. In 2013, he joined the Department of Electrical and Systems Engineering, University of Pennsylvania, Philadelphia, PA, USA, as a Research Scholar. Since 2016, he has been with Tsinghua University, where he is currently an Assistant Professor. He has authored or co-authored over 90 journal papers and 45 international conference papers. He holds 15 granted Chinese patents. His current research interests include metamaterials, plasmonics, electromagnetics, nanocircuits, mobile and handset antennas, MIMO and diversity antennas, and millimeter-wave antennas and arrays.

Dr. Li was a recipient of the Issac Koga Gold Medal from URSI General Assembly in 2017, the Second Prize of Science and Technology Award of China Institute of Communications in 2017, the Young Scientist Awards from the conferences of ACES 2018, AT-RASC 2018, AP-RASC 2016, EMTS 2016, URSI GASS 2014, the Best Paper Awards from the conferences of CSQRWC 2018, NCMMW 2018 and 2017, APCAP 2017, NCANT 2017, ISAPE 2016, and ICMMT 2016, the Outstanding Doctoral Dissertation of Beijing Municipality in 2013, and the Principal Scholarship of Tsinghua University in 2011. He is serving as the Associate Editor for the IEEE TRANSACTIONS ON ANTENNAS AND PROPAGATION and the IEEE ANTENNAS AND WIRELESS PROPAGATION LETTERS and COMPUTER APPLICATIONS IN ENGINEERING EDUCATION, and also serves as the Editorial Board of *Scientific Report*.

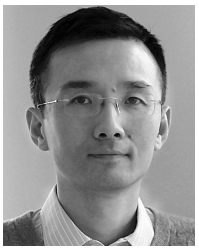

Zhijun Zhang (M'00–SM'04–F'15) received the B.S. and M.S. degrees from the University of Electronic Science and Technology of China, Chengdu, China, in 1992 and 1995, respectively, and the Ph.D. degree from Tsinghua University, Beijing, China, in 1999.

In 1999, he joined the Department of Electrical Engineering, University of Utah, Salt Lake City, UT, USA, as a Post-Doctoral Fellow, where he was appointed a Research Assistant Professor in 2001. In 2002, he was an Assistant Researcher with the University of Hawai'i at Mānoa, Honolulu, HI, USA, and a Senior Staff Antenna Development Engineer with Amphenol T&M Antennas, Vernon Hills, IL, USA, where he was promoted to Antenna Engineer Manager. In 2004, he joined Nokia Inc., San Diego, CA, USA, as a Senior Antenna Design Engineer. In 2006, he joined Apple Inc., Cupertino, CA, USA, as a Senior Antenna Design Engineer and was then promoted to Principal Antenna Engineer. Since 2007, he has been with Tsinghua University, where he is currently a Professor with the Department of Electronic Engineering. He has authored *Antenna Design for Mobile Devices* (Wiley, 1st ed. 2011, 2nd ed. 2017).

Dr. Zhang served as an Associate Editor for the IEEE TRANSACTIONS ON ANTENNAS AND PROPAGATIONfrom 2010 to 2014 and the IEEE ANTENNAS AND WIRELESS PROPAGATION LETTERS from 2009 to 2015.

Magdy F. Iskander (F'93–LF'12) was a Professor of electrical and computer engineering and the Engineering Clinic Endowed Chair Professor with the University of Utah, Salt Lake City, UT, USA. In 2002, he joined the University of Hawai'i at Mānoa, Honolulu, HI, USA, where he is currently a Professor of electrical engineering and the Director of the Hawaii Center for Advanced Communications, College of Engineering. He is also the Co-Director of the NSF Industry/University Cooperative Research Center with four other universities. He has authored or co-authored over 250 papers in technical journals, and has authored and edited several books, including the textbook *Electromagnetic Fields and Waves* (Prentice Hall, 1992, and Waveland Press, 2001; second edition 2012), and four books published by the Materials Research Society on *Microwave Processing of Materials*. He has made numerous presentations at national/international conferences. He holds nine patents. His current research interests include computational and biomedical electromagnetics and wireless communications was funded by the National Science Foundation, National Institute of Health, Army Research Office, U.S. Army CERDEC, Office of Naval Research, and several corporate sponsors.

Dr. Iskander was a recipient of many awards for excellence in research and teaching, including the University of Hawaii Board of Regents' Medal for Excellence in Research in 2013, the Board of Regents Medal for Teaching Excellence in 2010, the Hi Chang Chai Outstanding Teaching Award in 2011 and 2014, which is based on votes by graduating seniors, the IEEE MTT-S Distinguished Educator Award in 2013, the IEEE AP-S Chen-To Tai Distinguished Educator Award in 2012, the Richard R. Stoddard Award from the IEEE EMC Society in 1992, the Northrop Grumman Excellence in Teaching Award in 2010, the American Society for Engineering Education Curtis W. McGraw National Research Award in 1985, and the ASEE George Westinghouse National Award for Excellence in Education in 1991. He was the President of the IEEE Antennas and Propagation Society in 2002, and a Distinguished Lecturer and a Program Director of the Electrical, Communications, and Cyber Systems Division at the National Science Foundation. He has been the Founding Editor of the Computer Applications in *Engineering Education Journal* (Wiley), since 1992.